Phonon screening of excitons in atomically thin semiconductors

Supplemental Material

Woncheol Lee,[1] Antonios M. Alvertis,[2,3,4] Zhenglu Li,[4,3,5] Steven G. Louie,[3,4] Marina R. Filip,[6] Jeffrey B. Neaton,[3,4,7] and Emmanouil Kioupakis[8]

[1]Department of Electrical Engineering and Computer Science, University of Michigan, Ann Arbor, Michigan 48109, USA
[2]KBR, Inc. NASA Ames Research Center, Moffett Field, California 94035, United States
[3]Materials Sciences Division, Lawrence Berkeley National Laboratory, Berkeley, California 94720, USA
[4]Department of Physics, University of California Berkeley, Berkeley, California 94720, USA
[5]Mork Family Department of Chemical Engineering and Materials Science, University of Southern California, Los Angeles, California 90089, USA
[6]Department of Physics, University of Oxford, Oxford OX1 3PJ, United Kingdom
[7]Kavli Energy NanoScience Institute at Berkeley, Berkeley, 94720 California, USA
[8]Department of Materials Science and Engineering, University of Michigan, Ann Arbor, Michigan 48109, USA

1. Computational method

We performed first-principles calculations using density functional theory (DFT) and many-body perturbation theory (MBPT). We investigated a 20-atom wurtzite supercell structure consisting of atomically thin GaN quantum well with varying thickness (1 ML – 4 ML) embedded within AlN quantum barrier (FIG. S1). First, we performed structural relaxation calculation using local density approximation (LDA) for the exchange correlation functional [1-2], as implemented in Quantum ESPRESSO code [3]. Since the group-III nitrides require the $3d$ electrons for precise structural relaxations [4], we employed a norm-conserving pseudopotential of Ga, which include the $4s$, $4p$, and $3d$ electrons of Ga in the valence. Additionally, we fixed the in-plane lattice constant at the value of AlN ($a = 0.3112$Å) [5] and allowed atoms to move only along the polar c-axis of the supercell to mimic pseudo-morphic growth [6].

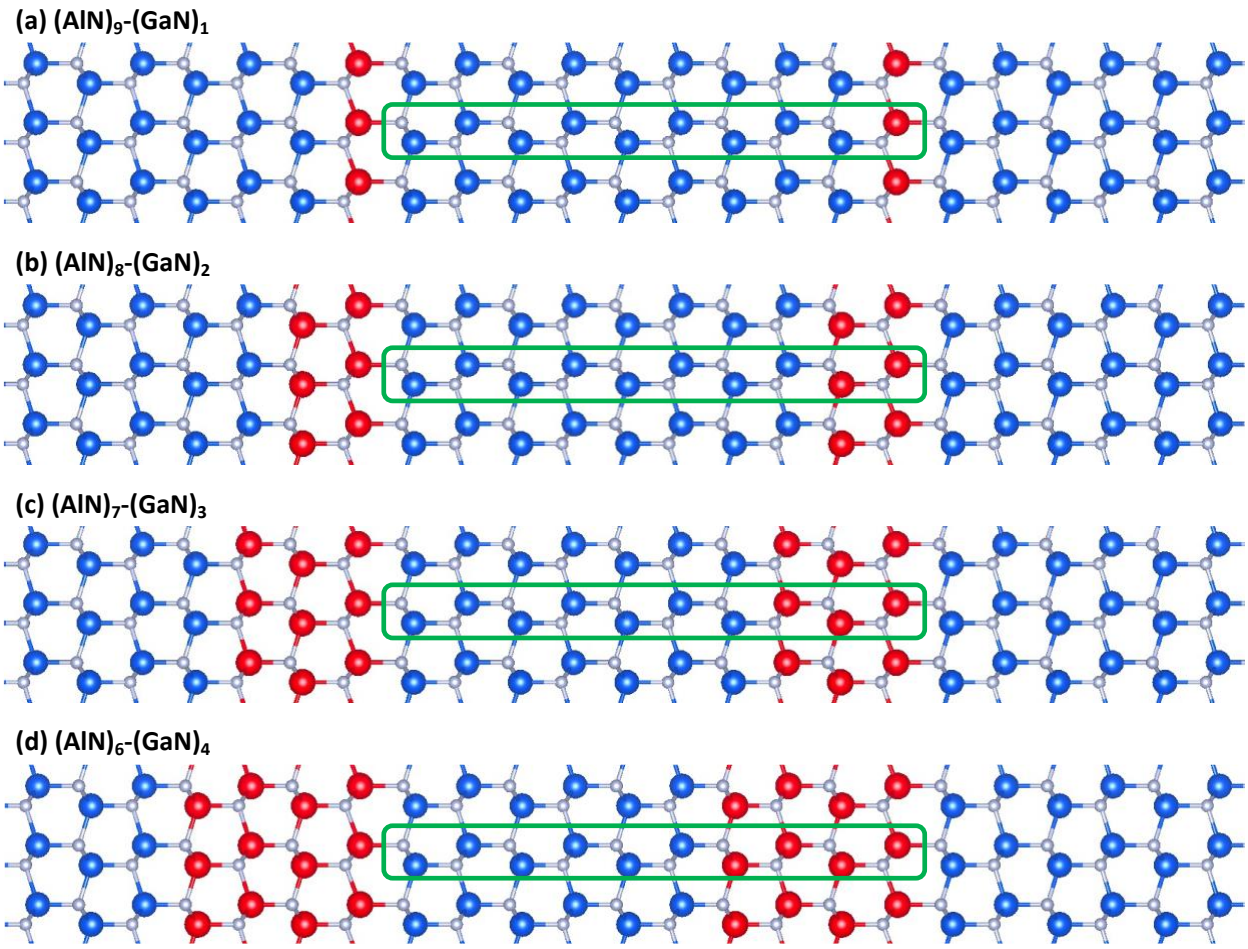

FIG. S1. Schematics of atomically thin GaN quantum wells with different thicknesses, embedded within AlN quantum barriers: (a) 1 ML GaN with 9 ML AlN, (b) 2 ML GaN with 8 ML GaN, (c) 3 ML GaN with 7 ML AlN, (d) 4 ML GaN with 6 ML AlN. The region highlighted by the green boundary represents the actual supercell employed in the DFT calculations. The circles in blue, red, and grey represent aluminum (Al), gallium (Ga), and nitrogen (N) atoms, respectively.

Next, we performed DFT calculations using Quantum Espresso [3]. We used a valence Ga pseudopotential that only consider $4s$ and $4p$ electrons to reduce the computation costs of the large-size supercell calculation. A planewave cutoff of 70 Ry with $8 \times 8 \times 1$ Monkhorst-Pack mesh converged the total energy of the supercell within 1mRy/atom.

Based on the DFT calculation, we calculated quasi-particle energy using G_0W_0 method, as implemented in the BerkeleyGW [7]. We used a screening cutoff energy of 20 Ry and $8 \times 8 \times 1$ Monkhorst-Pack mesh for the quasi-particle calculation. We chose plasmon-pole approximation to

calculate the frequency-dependent dielectric response [8]. Also, we adopted the static-remainder approach to accelerate the convergence over the number of unoccupied electron states [9].

Finally, we used BerkeleyGW to solve Bethe-Salpeter Equation (BSE) [10]:

$$\left(E^{\mathrm{QP}}_{c\mathbf{k}+\mathbf{Q}} - E^{\mathrm{QP}}_{v\mathbf{k}}\right)A^{S}_{vc\mathbf{k}} + \sum_{v'c'\mathbf{k}'} \left\langle vc\mathbf{k}\middle|K^{\mathrm{eh}}\middle|v'c'\mathbf{k}'\right\rangle A^{S}_{v'c'\mathbf{k}'} = \Omega^{S} A^{S}_{vc\mathbf{k}} \tag{1}$$

where $\mathbf{k}$ is an electron momentum, $\mathbf{Q}$ is an exciton center-of-mass momentum, c and v are conduction and valence band indexes, $E^{\mathrm{QP}}_{n\mathbf{k}}$ is a quasi-particle energy, $K^{\mathrm{eh}}_{vc;v'c'}$ is an electron-hole interaction kernel, $A^{S}_{vc\mathbf{k}}$ is an exciton wavefunction (i.e., electron-hole amplitude), and Ω^{S} is an exciton energy. In the calculations for 1 ML GaN and 2 ML GaN structures, we considered the lowest conduction band and the top three valence bands in the BSE calculation. In the case of 3 ML GaN and 4 ML GaN structures, we included the lowest conduction band and the top two valence bands. The same screening cutoff (20 Ry) was employed as in the quasiparticle calculation. For all cases, we use the patched sampling method [11] to interpolate the BSE kernel onto a Γ-centered patch of the Brillouin zone, drawn from a fine $140 \times 140 \times 1$ grid, converging the patch radius to ensure an accuracy of 10 meV or better for the exciton binding energy. After we obtain the exciton wavefunction ($A^{S}_{vc\mathbf{k}}$) from BSE calculations, we performed density-functional perturbation theory (DFPT) calculations to obtain the electron-phonon matrix [3]:

$$g_{ij,\nu}(\mathbf{k},\mathbf{q}) = \left\langle \psi_{i\mathbf{k}+\mathbf{q}}\middle|\Delta_{\mathbf{q}\nu}v^{\mathrm{KS}}\middle|\psi_{j\mathbf{k}}\right\rangle, \tag{2}$$

where i and j are band indexes, ν is a phonon branch index, $\mathbf{q}$ is a phonon momentum, $\psi_{i\mathbf{k}}$ is a Kohn-Sham wavefunction, and $\Delta_{\mathbf{q}\nu}v^{\mathrm{KS}}$ is a phonon-induced variation of the Kohn-Sham potential. We employ Wannier-Fourier interpolation [12] to obtain the electron-phonon matrix on the same fine patch as for the exciton wavefunction. We use modified versions of the Wannier90 [13] and EPW [14] codes, in order to ensure the gauge consistency of the electron-phonon matrix computed

from EPW and the exciton wavefunction obtained using BerkeleyGW. A detailed description of the computational workflow ensuring gauge consistency will be given elsewhere [15].

2. Absorption spectrum

Figure S2 shows the absorption spectra calculated for 1-4 MLs of GaN embedded within AlN barrier. Our calculation predicts a strong excitonic absorption peak appears in the deep UV range. We compare our calculated absorption spectra with experimentally measured photoluminescence spectra studied by several groups, thereby validating the reliability of our GW and BSE calculations.

For 1 ML (monolayer) GaN, which has been extensively studied due to its strong quantum confinement effect and deep-UV emission, multiple papers report a PL emission peak around 5.2-5.3 eV. This is consistent with our calculation results. Our simulated structure, with its in-plane lattice constant fixed to that of AlN to replicate actual pseudomorphic growth, shows the lowest 1s exciton peak at 5.28 eV (Figure S2a).

For 2 ML (bilayer) GaN, Refs. [16] and [17] reported a peak at 4.84-4.86 eV, which is slightly higher than our lowest 1s exciton peak at 4.58 eV (Figure S2, 2 ML GaN). This discrepancy may be due to thickness fluctuations in actual experiments, as discussed in Refs. [17] and [18], which is further evidenced by the relatively broad PL emission peak.

We denote that the absorption spectra calculations do not include phonon screening effects, which could renormalize the exciton binding energy as we discussed in the manuscript and cause slight shifts in the overall spectra.

References	Photoluminescence emission peak
[16] Y. Taniyasu and M. Kasu Appl. Phys. Lett. **99**, 251112 (2011)	0.9 ML GaN / 7.2 ML AlN: 5.23 eV 2 ML GaN / 8 ML AlN: 4.86 eV
[17] D. Bayerl *et. al.* Appl. Phys. Lett. **109**, 241102 (2016)	1 ML GaN / 7 ML AlN: 5.32 eV 2 ML GaN / 8 ML AlN: 4.84 eV
[18] A. Aiello *et. al.* Nano Lett. **19**, 7852−7858 (2019)	1 ML GaN / 10 nm AlN 5.18 – 5.28 eV
[19] A. A. Toropov et. al. Nano Lett. **20**, 158−165 (2020)	1 – 2ML GaN: 5.17 – 5.39 eV
[20] Y. Wu *et. al.* Appl. Phys. Lett. **116**, 013101 (2020)	1 ML GaN / 2 – 20 AlN: 4.9 – 5.25 eV

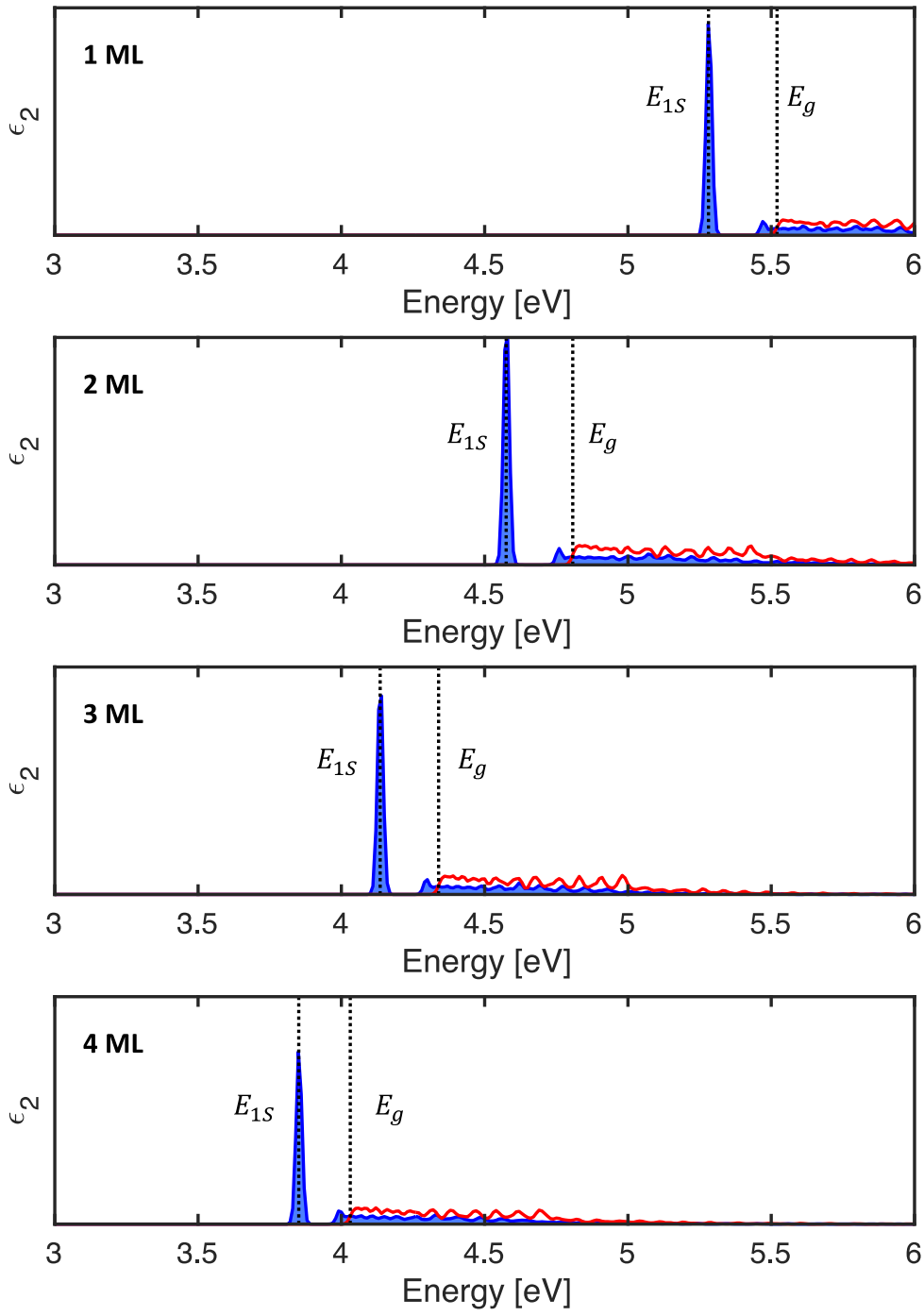

FIG. S2. Optical absorption spectra of atomically thin GaN with varying thicknesses. The blue shaded area indicates the spectra obtained from BSE, while the grey line represents the spectra obtained from random phase approximation (RPA). Vertical dashed lines indicate the energy of the lowest 1s exciton state (E_{1s}) from BSE calculations and the quasi-particle gap (E_g) obtained from G_0W_0 calculations.

3. Exciton binding energy obtained from the inclusion of phonon screening

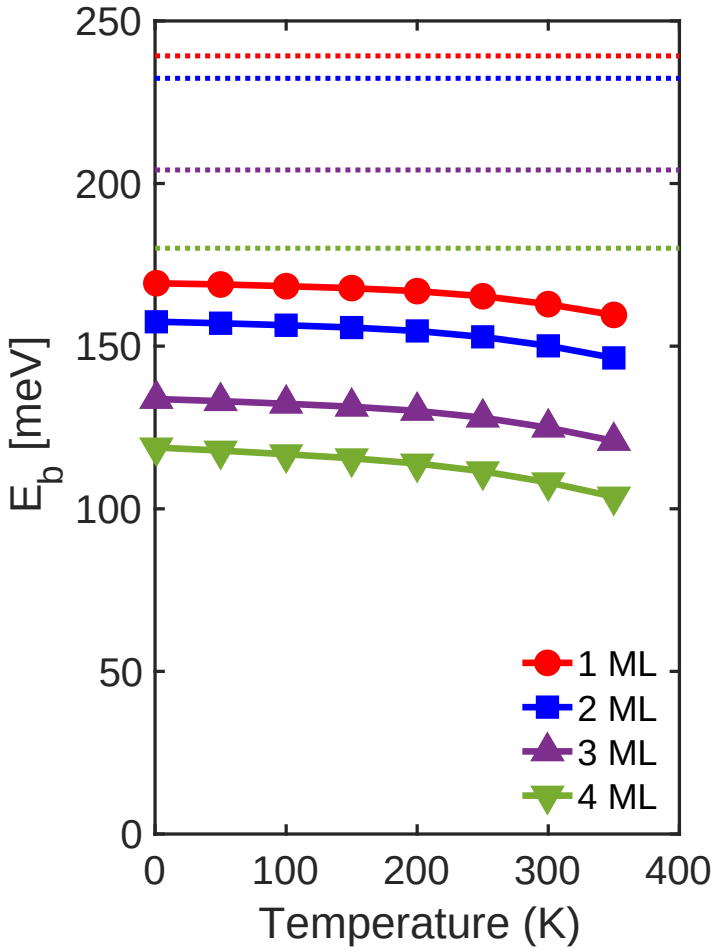

FIG. S3. Exciton binding energy calculated by the inclusion of the phonon screening effect (solid lines with symbols). Horizontal dashed lines indicate the exciton binding energy of four different GaN quantum wells, as determined from standard BSE calculation (without the inclusion of phonon screening).

4. Electron-phonon matrix

(a) LO phonon (Fröhlich interaction)

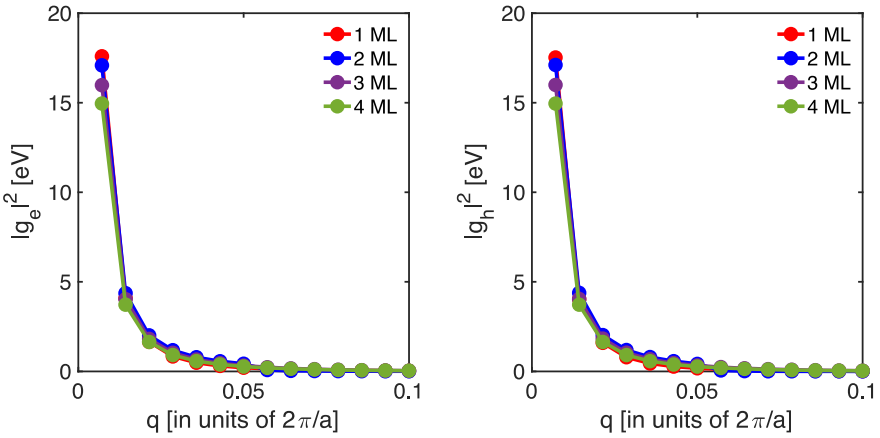

(b) LA phonon (Piezoelectric interaction)

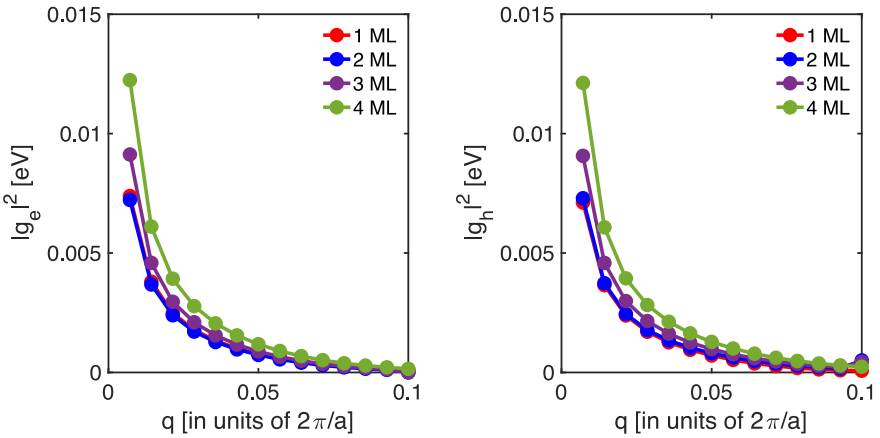

(c) HS phonons

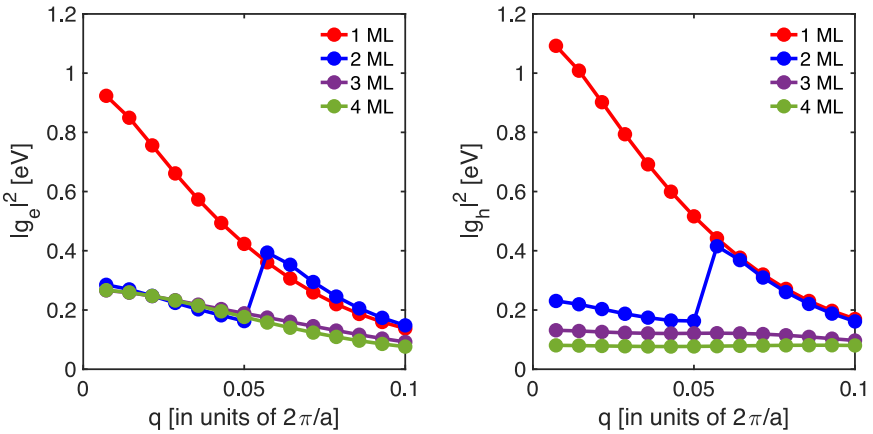

FIG. S4. Electron-phonon matrix $g_{cc',\nu}(\boldsymbol{k}=\Gamma,\boldsymbol{q})$ and hole-phonon matrix $g_{vv',\nu}(\boldsymbol{k}=\Gamma,\boldsymbol{q})$ for different vibrational modes. The discontinuity observed in the case of 2 ML arises from the crossing between LO and HS modes in the phonon dispersion.

5. Phonon eigenvector

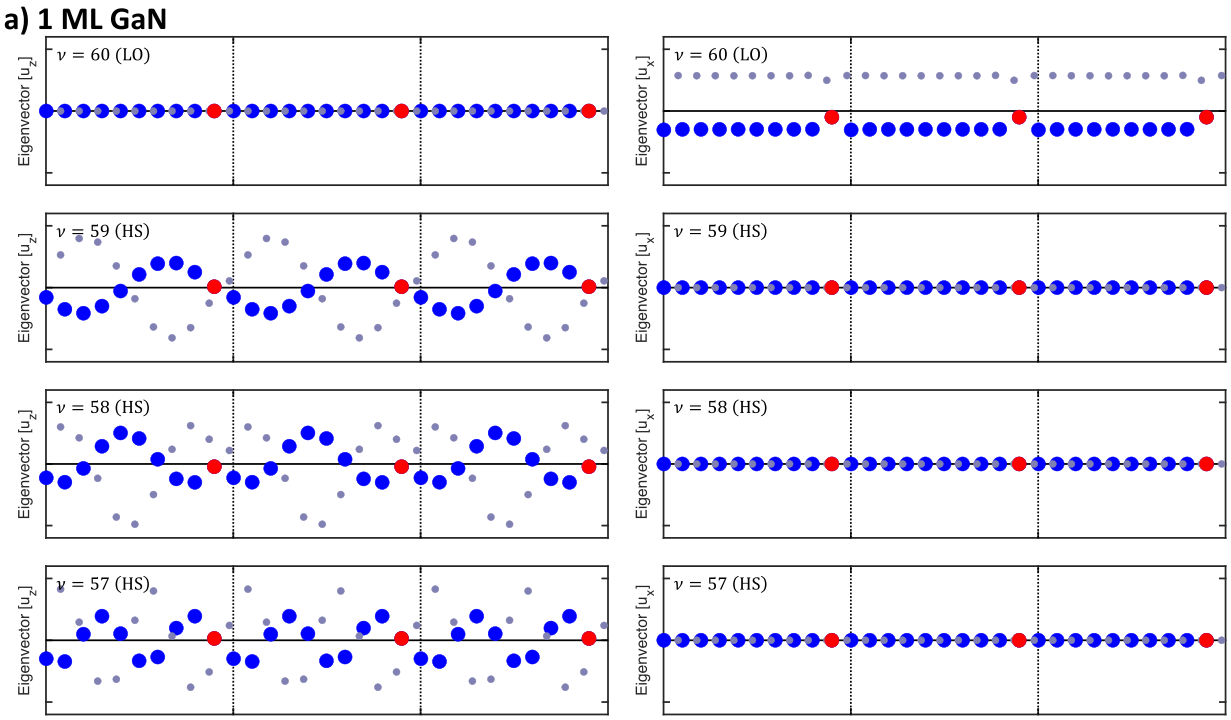

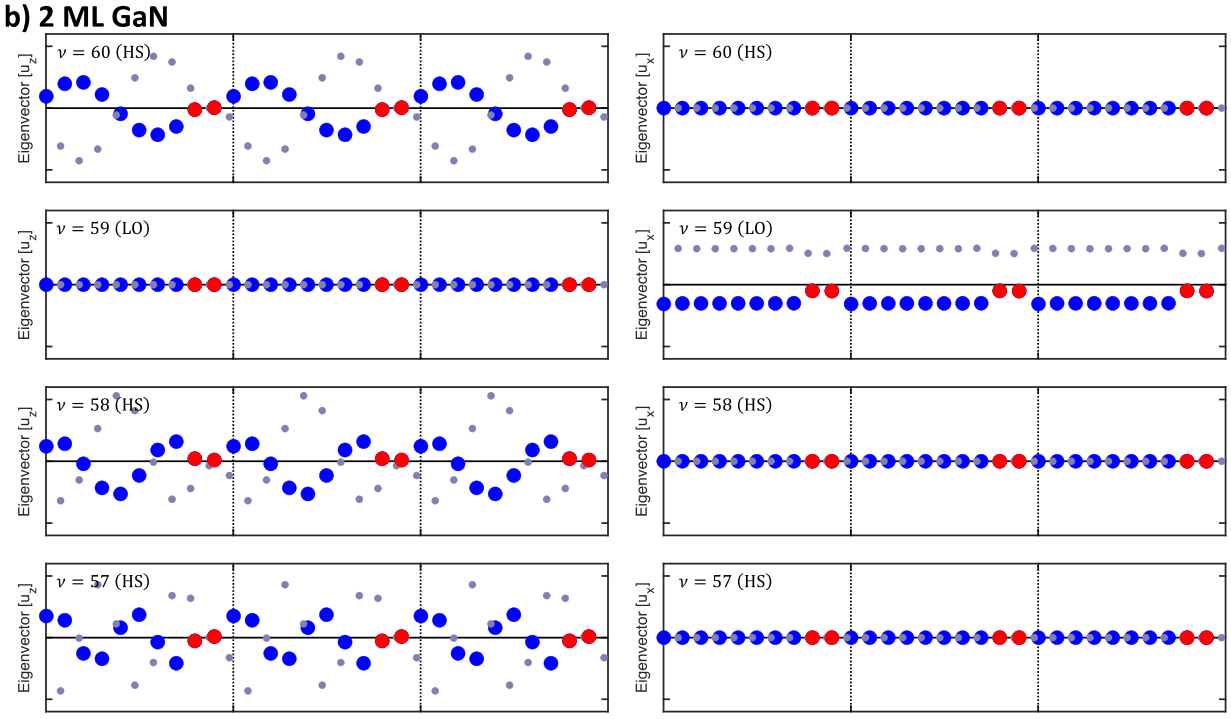

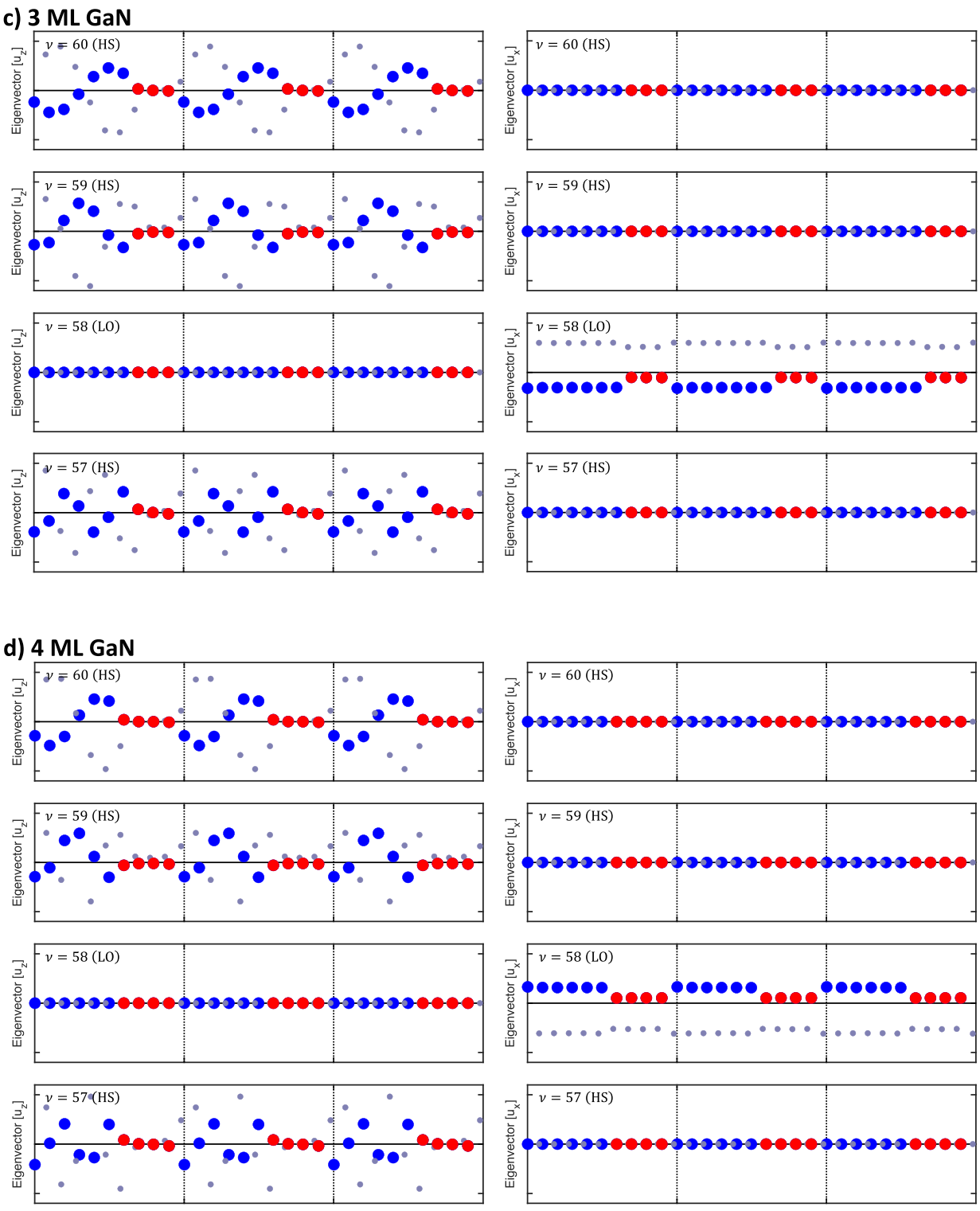

FIG. S5. Phonon eigenvectors shown for the LO phonon modes vibrating along the in-plane direction and the HS modes vibrating along the z-axis. For brevity, we are presenting only the four highest-energy phonon modes at $\boldsymbol{q} = 0$.

6. Phonon dispersion

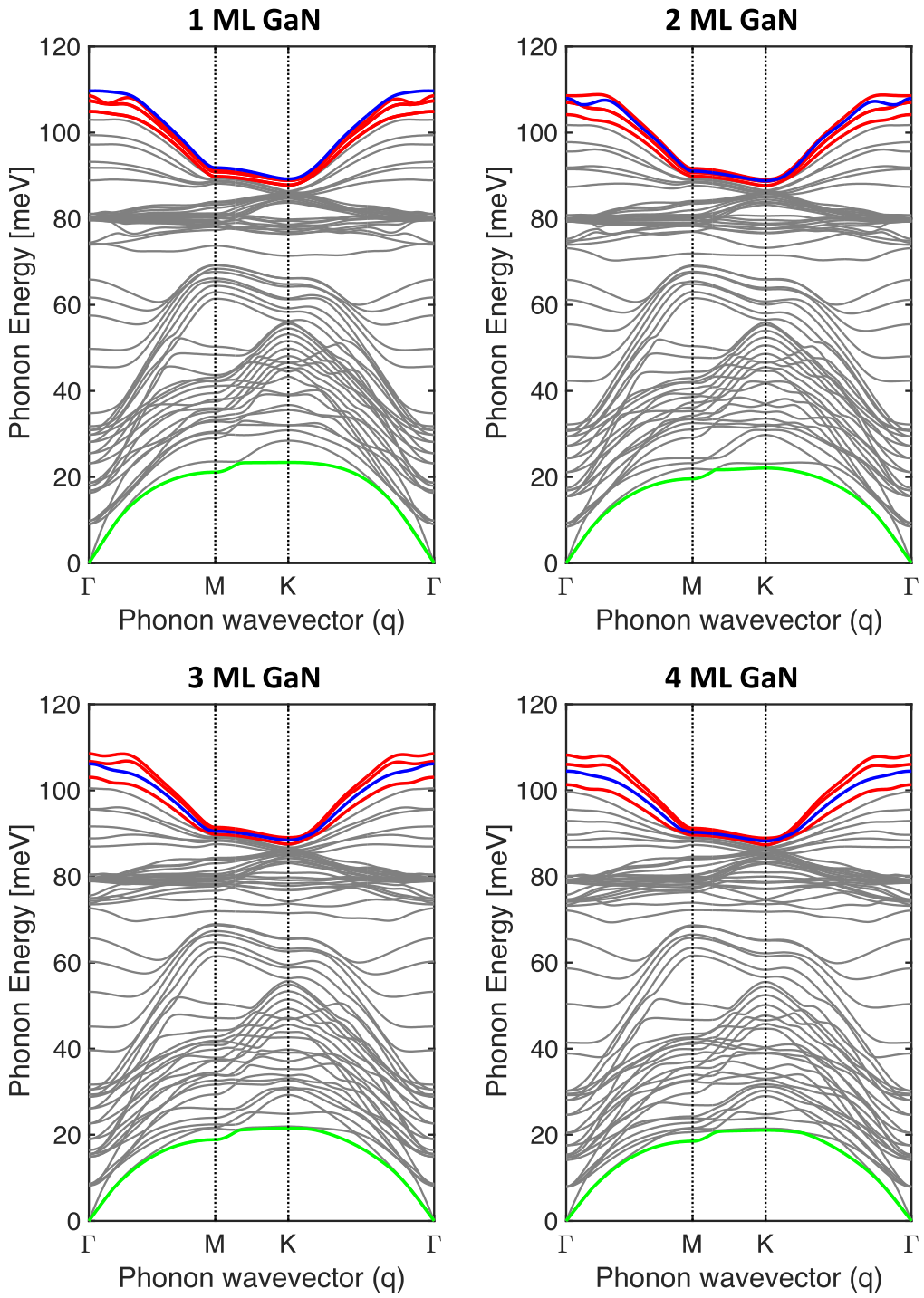

FIG. S6. Phonon dispersion of four different supercells, each with varying GaN quantum well thickness. The blue curve illustrates the Fröhlich-type LO phonon mode in the in-plane direction, the red curves indicate three HS phonon modes shown in Fig. S3, and the green curve represents the piezoelectric LA phonon mode.

7. Electron and hole wavefunctions

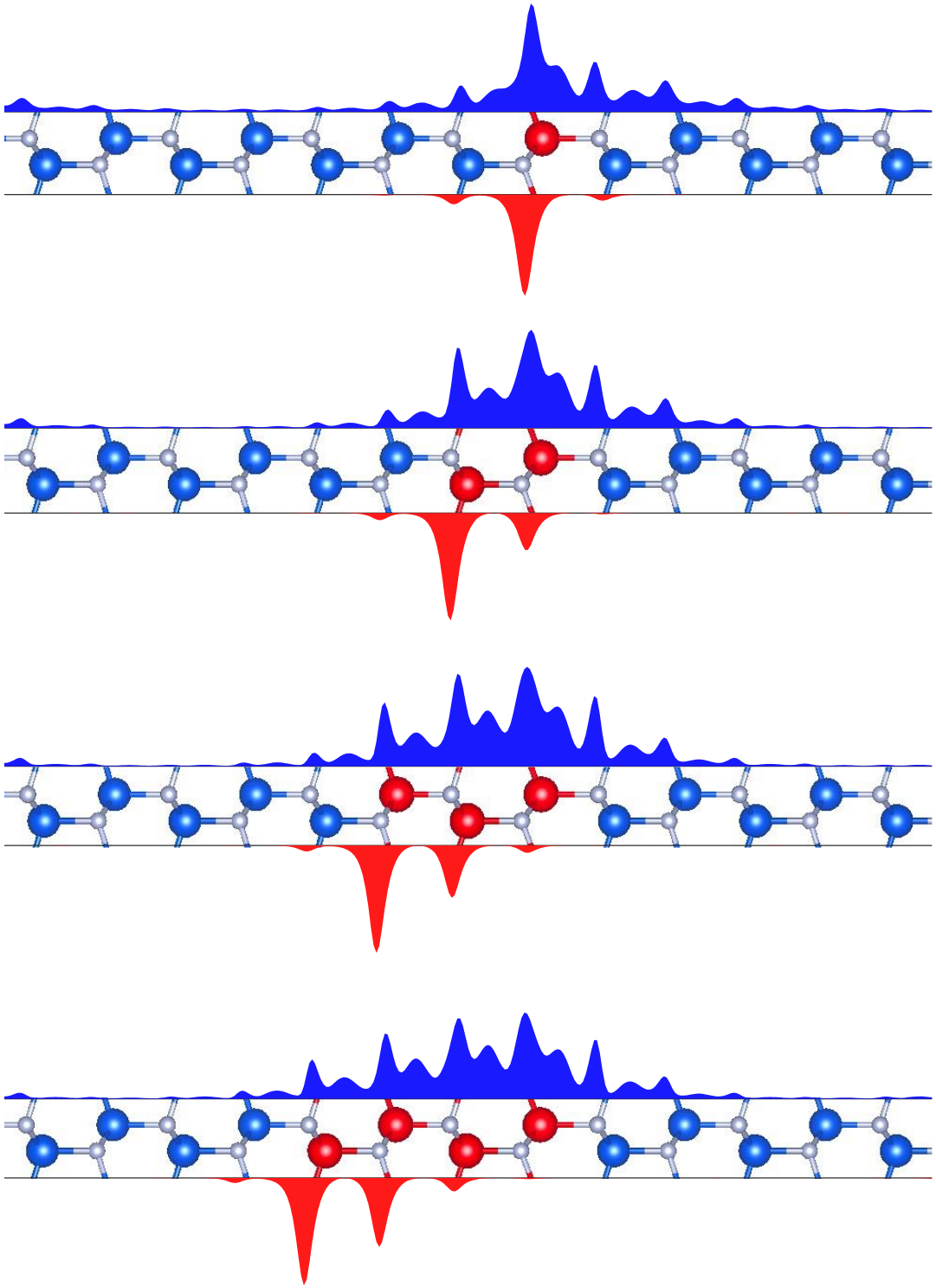

FIG. S7. Electron wavefunction (blue) and hole wavefunction (red) for 1-4 ML GaN quantum wells

8. Exciton wavefunction $A_{vc\mathbf{k}}$ in reciprocal space

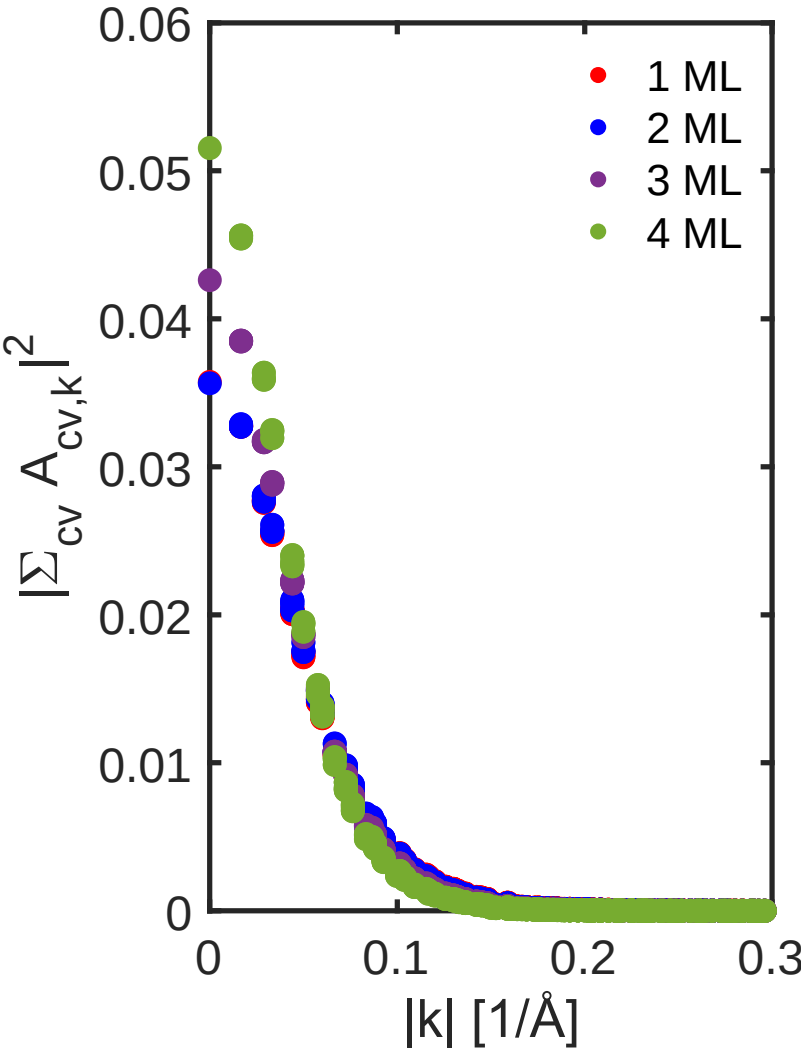

References

[1] D. M. Ceperley and B. J. Alder, "Ground State of the Electron Gas by a Stochastic Method," *Phys. Rev. Lett.*, vol. 45, no. 7, pp. 566–569, Aug. 1980.

[2] J. P. Perdew and A. Zunger, "Self-interaction correction to density-functional approximations for many-electron systems," *Phys. Rev. B*, vol. 23, no. 10, pp. 5048–5079, May 1981.

[3] P. Giannozzi *et al.*, "Advanced capabilities for materials modelling with Quantum ESPRESSO," *J. Phys. Condens. Matter*, vol. 29, no. 46, p. 465901, Nov. 2017.

[4] C. Stampfl and C. G. Van de Walle, "Density-functional calculations for III-V nitrides using the local-density approximation and the generalized gradient approximation," *Phys. Rev. B*, vol. 59, no. 8, pp. 5521–5535, Feb. 1999.

[5] W. M. Yim, E. J. Stofko, P. J. Zanzucchi, J. I. Pankove, M. Ettenberg, and S. L. Gilbert, "Epitaxially grown AlN and its optical band gap," *J. Appl. Phys.*, vol. 44, no. 1, pp. 292–296, 1973.

[6] A. Aiello *et al.*, "Deep Ultraviolet Luminescence Due to Extreme Confinement in Monolayer GaN/Al(Ga)N Nanowire and Planar Heterostructures," *Nano Lett.*, vol. 19, no. 11, pp. 7852–7858, 2019.

[7] J. Deslippe, G. Samsonidze, D. A. Strubbe, M. Jain, M. L. Cohen, and S. G. Louie, "BerkeleyGW: A massively parallel computer package for the calculation of the quasiparticle and optical properties of materials and nanostructures," *Comput. Phys. Commun.*, vol. 183, no. 6, pp. 1269–1289, 2012.

[8] M. S. Hybertsen and S. G. Louie, "Electron correlation in semiconductors and insulators: Band gaps and quasiparticle energies," *Phys. Rev. B*, vol. 34, no. 8, pp. 5390–5413, Oct. 1986.

[9] J. Deslippe, G. Samsonidze, M. Jain, M. L. Cohen, and S. G. Louie, "Coulomb-hole summations and energies for *GW* calculations with limited number of empty orbitals: A modified static remainder approach," *Phys. Rev. B*, vol. 87, no. 16, p. 165124, Apr. 2013.

[10] M. Rohlfing and S. G. Louie, "Electron-hole excitations and optical spectra from first principles," *Phys. Rev. B*, vol. 62, no. 8, pp. 4927–4944, Aug. 2000.

[11] D. Y. Qiu, F. H. da Jornada, and S. G. Louie, *Screening and Many-Body Effects in Two-Dimensional Crystals: Monolayer MoS_2*, Phys. Rev. B **93**, 235435 (2016).

[12] F. Giustino, M. L. Cohen, and S. G. Louie, *Electron-Phonon Interaction Using Wannier Functions*, Phys. Rev. B **76**, 165108 (2007).

[13] G. Pizzi et al., *Wannier90 as a Community Code: New Features and Applications*, J. Phys. Condens. Matter **32**, 165902 (2020).

[14] S. Poncé, E. R. Margine, C. Verdi, and F. Giustino, *EPW: Electron–Phonon Coupling, Transport and Superconducting Properties Using Maximally Localized Wannier Functions*, Comput. Phys. Commun. **209**, 116 (2016).

[15] Z. Li, A. M. Alvertis, S. Gant, J. B. Neaton, and S. G. Louie, *Wannier-function-assisted many-body GW-Bethe-Salpeter equation calculations: Gauge consistency involving phonons, nonuniform sampling, and ground-state starting point*, to be submitted (2023).Z. Li, A. M. Alvertis, S. E. Gant, J. B. Neaton, and S. G. Louie, In preparation

[16] Y. Taniyasu and M. Kasu, *Polarization Property of Deep-Ultraviolet Light Emission from C-Plane AlN/GaN Short-Period Superlattices*, Appl. Phys. Lett. **99**, 251112 (2011).

[17] D. Bayerl, S. Islam, C. M. Jones, V. Protasenko, D. Jena, and E. Kioupakis, *Deep Ultraviolet Emission from Ultra-Thin GaN/AlN Heterostructures*, Appl. Phys. Lett. **109**, 241102 (2016).

[18] A. Aiello et al., *Deep Ultraviolet Luminescence Due to Extreme Confinement in Monolayer GaN/Al(Ga)N Nanowire and Planar Heterostructures*, Nano Lett. **19**, 7852 (2019).

[19] A. A. Toropov et al., *Strongly Confined Excitons in GaN/AlN Nanostructures with Atomically Thin GaN Layers for Efficient Light Emission in Deep-Ultraviolet*, Nano Lett. **20**, 158 (2020).

[20] Y. Wu, X. Liu, P. Wang, D. A. Laleyan, K. Sun, Y. Sun, C. Ahn, M. Kira, E. Kioupakis, and Z. Mi, *Monolayer GaN Excitonic Deep Ultraviolet Light Emitting Diodes*, Appl. Phys. Lett. **116**, 013101 (2020).